

Possible mineral sources of magnetic anomalies on Mars

G. KLETETSCHKA and N. F. NESS, Bartol Research Institute at Delaware University, Newark, U.S.

P. J. WASILEWSKI, J. E. P. CONNERNEY, and M. H. ACUNA, Goddard Space Flight Center, NASA, Greenbelt, U.S.

At the end of the last millennium, numerous (USSR and U.S.) spacecraft were sent to Mars to begin exploration of that planet. Mars Global Surveyor (1997 onward) is one of the successful missions that provided a detailed map of the topography and high resolution images of the surface, and also discovered unusually large remanent magnetism of the crust (up to 20 times larger than terrestrial standards).

The present-day anomalies indicate that Mars had at one time its own internal source of a planetary magnetic field from a magnetic dynamo resulting from motions of highly electrically conducting core material—similar to the dynamo that produces today's main magnetic field on Earth. Crustal rocks were cooled, perhaps metamorphosed, and became magnetized by the dynamo-generated magnetic field.

Relative timing of magnetic crust on Mars. The two physiographic regions on Mars, the Southern Highlands and Northern Lowlands, define the crustal dichotomy between the southern and the northern hemispheres. This dichotomy is also reflected in crustal thickness and surface geology. Most magnetic anomalies detected by MGS are in the Southern Hemisphere within the Southern Highlands (Figure 1). The amplitude of many Southern Highland anomalies is over 10 times what is observed on Earth at the same 400-km altitude. The presence of coherent magnetic anomalies occupying large regions indicate the past dynamo field but what about those regions where the magnetism is small or absent?

The absence of magnetism indicates that the underlying crust was either formed and/or modified (igneous and/or metamorphic) after the magnetic dynamo had ceased. These events may represent remelting and/or reheating of large portions of the crust by rock-forming processes or by impact-related demagnetization or physical removal of magnetized crustal material. The magnetic anomaly distribution outlines two different age epochs of Mars crust. The oldest crust (>3 billion years) is associated with the significant magnetic anomalies (greater than 15–20 nT at 400 km altitude) and the younger modified crust with magnetic signatures less than 15 nT to lower than the instrument detection threshold (± 4 nT).

Magnetizing mechanisms. Minerals contained within the cooling Martian crust were magnetized by the ambient magnetic field. Two distinct mechanisms allow homogenous magnetizations of large volumes of rocks within the crust at temperatures dependent on the particular mineral—commonly around 500°C. Mechanism 1 is acquisition of thermoremanent magnetization (TRM) by the magnetic minerals cooling and passing through the mineral-specific blocking temperatures. Mechanism 2 is acquisition of chemical remanent magnetization (CRM) which can occur also during cooling. However, in the case of CRM, the magnetic minerals are formed below their blocking temperatures as a result of the new phase precipitation, for example, during the phase exsolution processes.

Both processes are very efficient and comparable in the resulting TRM intensity acquired just below the blocking temperature of the grains. At the blocking temperatures the magnetic moment of the grain is forced by the ambient magnetic field to be parallel to the applied field. Several degrees below this temperature, the stability of the magnetic moment against magnetic changes increases exponentially and information

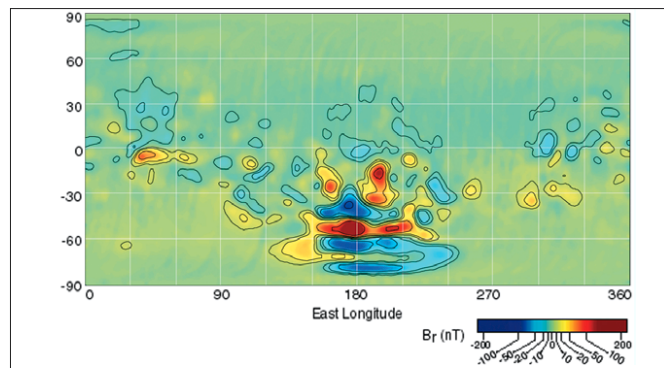


Figure 1. Radial field component of magnetic anomalies on Mars. Vertical and horizontal axes are latitude and longitude, respectively. The data plotted were obtained in the night side of the planet at 400-km altitude. Radial component in this diagram is opposite in sign with respect to Z-component magnetic anomalies, more customary in Earth exploration.

about the ambient field becomes frozen within the mineral grains. In the case of CRM, the new magnetic phase starts to nucleate at a subnanometer size. In this state, the magnetic moment of the grain is perturbed by thermal fluctuations and the blocking temperature of the grain is very low. With increasing size of the nucleating grain, the blocking temperature rises. Because the CRM has, by definition, blocking temperatures above the temperature of the precipitate, the blocking temperature of the growing grain must, at some point, reach the precipitating temperature. At this growth stage, the grain records the ambient magnetic field and further growth will contribute to further stabilization of the CRM.

Available magnetic minerals. Only a few magnetic minerals can be responsible for magnetic anomalies on Mars. Attempts were made to assess the nature of the magnetic minerals in the Martian soil (Viking and Pathfinder missions) by collecting small magnetic particles with strong magnets that were part of the experiment packages on the Viking (1976) and Pathfinder (1996) landers. This resulted in a list of potential magnetic mineral candidates—notably metallic iron, magnetite and/or titanomagnetite, maghemite, and monoclinic pyrrhotite. All these minerals have high magnetic susceptibility; this equipment yields no information about lower susceptibility minerals such as hematite, and goethite as they would not be attracted by the magnet arrays.

The sources of remanent magnetism do not necessarily constitute the same spectrum of magnetic minerals sampled by the lander mission magnet arrays. Magnets attract high susceptibility minerals that may not have the potential to hold a stable remanence. In this note we evaluate the class of magnetic minerals that may represent the sources of remanent magnetization for these anomalously large planetary magnetic anomalies.

Among the common rock-forming minerals, only a few are capable of acquiring and retaining significant remanent magnetization. These minerals are among the oxides and sulfides, which are commonly found on Earth. The available petrographic data for the SNC meteorites, inferences based on soil analyses, magnetic experiments on the Viking and Pathfinder missions, and inference based on the Thermal Emission Spectrometer suggest that magnetite, hematite, and

Table 1. Ward collection of natural rocks

ward sample	ward collection	mass [g]	NRM [A/m]	SIRM [A/m]	ward sample	ward collection	mass [g]	NRM [A/m]	SIRM [A/m]
1 Biotite granite, Barre, Vermont		7.05	0.0	0.3	48 Glauconitic sandstone, Hazlet, New Jersey		7.74	0.0	3.3
2 Muscovite granite, Concord, New Hampshire		9.85	0.0	0.0	49 Siltstone, Near Newhall, California		7.02	0.0	0.1
3 Biotite hornblende granite, St Cloud, Minnesota		5.94	0.0	0.4	50 Arkose, Mt. Tom, Massachusetts		7.83	0.0	4.5
4 Alcaic granite, Quincy, Massachusetts		7.4	0.0	1.2	51 Graywacke, Grafton, New York		7.07	0.0	0.2
5 Aplitic, Boulder Co., Colorado		6.96	0.0	1.5	52 Argillaceous shale, Rochester, New York		10	0.0	0.0
6 Quartz monzonite porphyry, Garfield, Colorado		8.79	0.1	16.6	53 Araneous shale, Greene County, New York		6.3	0.0	1.3
7 Granodiorite, St. Cloud, Minnesota		7.76	1.7	38.7	54 Oil shale, Garfield County, Colorado		23.5	0.0	0.0
10 Rhyolite Tuff, Frying Pan Basin, Montana		14	0.0	1.7	55 Bauxite, Bauxite, Arkansas		5.69	5.5	57.6
11 Rhyolite, Castle Rock, Colorado		7.3	0.1	4.7	57 Siliceous oolite, State College, Pennsylvania		28	0.0	0.1
12 Rhyolite porphyry, Chaffee Co., Colorado		4.24	0.4	38.0	59 Enclinal limestone, Lockport, New York		32.1	0.0	0.1
13 Hornblende syenite, Cuttingsville, Vermont		9.84	0.0	16.5	60 Limestone, Fremont County, Colorado		28.9	0.0	4.4
14 Alcaic syenite, Cripple Creek, Colorado		7.09	0.7	173.9	61 Cherty limestone, LeRoy, New York		23.5	0.0	0.0
15 Trachyte porphyry (bostonite), Essex County, New York		8.52	0.0	5.8	62 Oolitic limestone, Tyrone, Pennsylvania		28.8	0.0	0.6
16 Trachyte porphyry, Cripple Creek, Colorado		7.25	0.0	11.0	63 Chalk, Oktibeha Co., Mississippi		23.3	0.0	0.0
17 Nepheline Syenite, Blue Mt., Methuen Twp, Ontario		8.76	0.0	0.8	64 Calcerous tufa, Murnford, New York		18.9	0.0	0.0
18 Nepheline-sodalite syenite, Red Hill, New Hampshire		8.1	0.1	151.5	65 Dolomitic limestone, Rochester, New York		25.2	0.0	0.1
19 Ijolite, McClure Mountain, Colorado		5.96	2.3	28.8	67 Hematite limestone, Wayne County, New York		7.4	0.1	117.0
20 Siderite carbonate, Iron Hill, Colorado		12.1	0.0	0.1	68 Siderite rock, Negaunee, Michigan		39.6	1.5	659.7
21 Phonolite, Cripple Creek, Colorado		4.1	0.2	38.7	72 Marble (pink), Tate, Georgia		31.1	0.0	0.0
22 Monzonite, Silverton, Colorado		7.1	0.7	153.7	73 Dolomite marble, Thornwood, New York		29	0.0	0.0
23 Lattie Porphyry, Bear Paw Mountains, Montana		7.9	2.2	81.5	74 Verde antique (serpentine), Rochester, Vermont		27.4	1.5	231.2
24 Tonalite (quartz diorite), San Diego County, California		7.01	0.0	0.4	75 Garnet wollastonite skarn, Willsboro, New York		37	0.0	0.0
25 Diorite, Los Angeles County, California		9.41	0.0	4.0	77 Slate (gray) Bangor, Pennsylvania		30	0.0	0.0
26 Dacite, N. W. of Helena, Montana		5.73	0.2	21.1	78 Phyllite, Ely, Orange County, Vermont		2.45	0.1	2.9
27 Hornblende andeste, Mt. Shasta, California		6.97	4.3	133.9	79 Mica schist, Manhattan, New York		6.13	0.6	44.1
28 Hornblende gabbro, San Diego Co., California		8.7	3.9	214.3	80 Chlorite schist, Chester, Vermont		8.92	0.5	124.6
29 Norite, Wollaston Twp., Ontario		10.2	13.7	249.2	81 Stilpnomelane schist, Mendocino County, California		36.7	0.0	0.0
30 Olivine gabbro, Wichita Mountain, Oklahoma		11.3	0.5	706.7	82 Talc-Tremolite schist, St. Lawrence County, New York		34.8	0.0	0.0
31 Hornblende gabbro, Salem, Massachusetts		9.02	1.1	94.4	83 Graphite schist, Warren County, New York		7.4	0.0	0.8
32 Anorthosite, Elizabethtown, New York		9.76	0.0	0.5	84 Andalusite (chastolite) slate, Mariposa Co., California		7.68	0.0	0.6
33 Diabase, Jersey City, New Jersey		8.82	0.4	21.0	85 Staurolite quartzite, Petaca, New Mexico		34.6	7.7	720.7
34 Scoria, Klamath Falls, Oregon		3.46	11.4	281.1	86 Kyanite quartzite, Near Ogilby, California		14.6	0.0	0.1
35 Amygdaloidal Basalt, Keweenaw County, Michigan		7.5	2.6	296.1	87 Sillimanite-garnet gneiss, Warren County, New York		8.03	0.0	0.1
36 Basalt, Chimney Rock, New Jersey		9.22	5.8	620.5	88 Cordierite anthophyllite skarn, Guffey, Colorado		13.1	0.0	0.3
37 Olivine basalt porphyry, Valmont, Colorado		10.1	3.7	205.7	89 Augen gneiss, St. Lawrence Co., New York		8.57	0.4	3802.5
38 Diabase porphyry, Cape Ann, Massachusetts		8.73	0.3	23.5	90 Granitoid gneiss, Salisbury, North Carolina		7.17	0.0	471.7
39 Lamprophyre, Spanish Peaks, Colorado		11.2	12.9	342.4	91 Biotite gneiss, Uxbridge, Massachusetts		7.64	0.0	19.9
40 Pyroxenite (Hartzburgite) Stillwater Complex, Montana		9.54	0.1	37.2	92 Eclogite, Sonoma County, California		16.8	0.0	0.3
41 Dunite (Olivine Peridotite), Balsam, North Carolina		8.7	0.0	2.5	93 Actinolite Schist, Chester, Vermont		5.25	0.0	1.0
42 Kimberlite, Muftreesboro, Arkansas		15.7	0.0	0.2	94 Cummingtonite schist, Leeds, South Dakota		5.97	0.1	28.9
44 Quartz-pebble conglomerate, Nanticoke, Pennsylvania		8	0.0	0.1	95 Hornblende schist, Mitchell Co., North Carolina		10.5	0.0	0.1
45 Gray sandstone, Berea, Ohio		6.5	0.0	0.4	96 Glaucophane schist, Sonoma County, California		6.65	0.0	0.0
46 Red sandstone, Potsdam, New York		28.2	0.0	1.3	97 Hornblende gneiss, Clintonville, New York		10.4	0.0	0.3

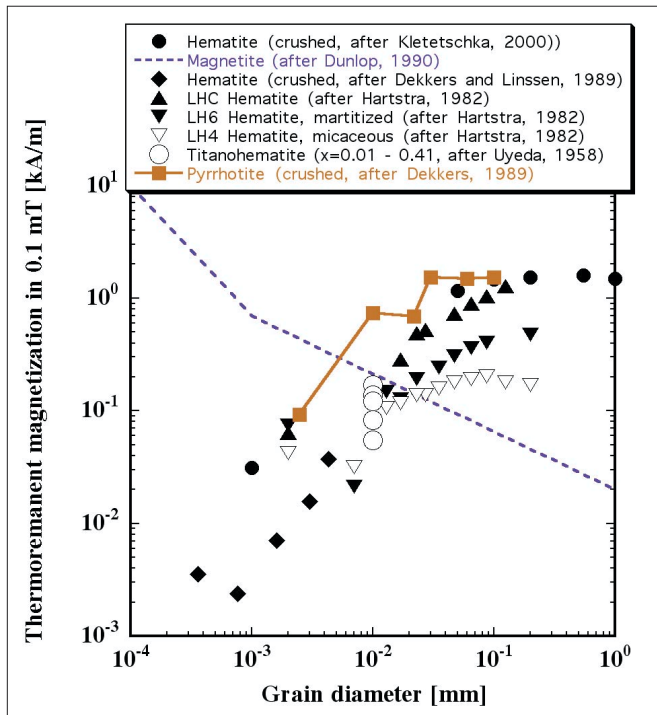


Figure 2. TRM magnetizations for the three main candidate minerals that can constitute the source of the magnetic anomalies on Mars.

pyrrhotite are the primary candidate minerals to be considered. Minerals, such as low-Ti titanomagnetites and titanohematites, similar to the magnetites and hematites, respectively, need not be considered separately.

Rocks with maximum magnetization. Intense magnetic crustal sources, detected in the Terra Sirenum region (120°W to 210°W; 30°S to 85°S), require an estimated magnetic moment of $\sim 1.3 \times 10^{17}$ A m². For a 30-km magnetized layer, this moment translates to a magnetization of ~ 20 A/m. It can be assumed that initially this magnetization was acquired as a TRM/CRM, because these are the only remanence acquiring mechanisms operating in the deep crustal rocks. Table 1 shows an example of common values for remanent magnetizations acquired in geomagnetic field by common terrestrial rocks (NRM column). The maximum possible magnetization of these specimens is also shown (SIRM column). This data set indicates that it is quite exceptional for terrestrial rocks to have a magnetization of 20 A/m, apart from the large volumes required (30-km layer) with uniform magnetization.

The magnetization of hematite, magnetite, and pyrrhotite in their pure form changes according to grain size (Figure 2, note that the unit is kA/m). The diagram (the acquisition field is 0.1 mT) indicates that the maximum possible TRM of large grains of hematite and pyrrhotite is a little more than 1000 A/m. Magnetization for small grains of magnetite is close to 10 000 A/m. Both hematite and pyrrhotite can acquire strong magnetization while in large grain size. Thus, maximum intensity per volume of the rock formation occurs when hematite and pyrrhotite accumulate by ore-forming processes. In such a case the concentration of hematite and/or pyrrhotite can be >50% (by volume) and magnetization of the entire rock can be greater than 500 A/m.

Magnetite can be more magnetic (by almost an order of magnitude) but only when small in grain size. There is only one mechanism that can preserve the small grain size of magnetite in deep crustal rocks. This mechanism is an exsolution from silicate minerals. Exsolution of fine grained magnetite

permits only about a half percent (by volume) concentration due to problems of fitting magnetite in the host-phase crystal-lattice defects and due to a change from the phase hosting Fe that has to be compensated. This limits the maximum overall magnetization of rocks with magnetite (0.5% by volume) to about 50 A/m, an order of magnitude lower than magnetizations of hematite and pyrrhotite.

All three minerals—magnetite, hematite, and pyrrhotite—can generate enough magnetization to produce the observed magnetic anomalies. There must be a way to enhance the concentration of one of these minerals within large volumes of Martian crust while keeping a uniform magnetizing direction. As discussed before, ore deposits are one way of making possible large volumes of large magnetization regions. This is directly connected to the early history formation of the crust and choosing one of these minerals over the other will have major impact on the evolution path of Martian crust. Hematite presence in lower crustal Martian rocks would imply high oxidation levels. The occurrence of hematite-bearing lower crustal rocks on Earth may be attributed to the orogenic recycling of oxidized surface material, a process for which there is so far no clear evidence on Mars. Both magnetite and pyrrhotite have been detected in SNC meteorites. Lower crust with large concentration of magnetite requires a special mechanism to disperse fine-grained magnetite, and/or produce complex textures so the magnetization can be stable and survive more than three billion years. Pyrrhotite rich crust would imply large hydrothermal flows accumulating enough pyrrhotite concentration in a massive form.

Suggested reading. *Rock Magnetism—Fundamental and Frontiers* by Dunlop and Ozdemir (Cambridge Studies in Magnetism, 1997). “Unique thermoremanent magnetization of multidomain sized hematite: Implications for magnetic anomalies” by Kletetschka et al. (*Earth and Planetary Science Letters*, 2000). “Mineralogy of the sources for magnetic anomalies on Mars” by Kletetschka et al. (*Meteoritics and Planetary Science*, 2000). “Pyrrhotite and the remanent magnetization of SNC meteorites: a changing perspective on Martian magnetism” by Rochette et al. (*Earth and Planetary Science Letters*, 2001). [TJE](#)

Acknowledgments: We thank Dhananjay (Tiku) Ravat for discussions. We are grateful to NASA for the support of our research.

Gunther Kletetschka is a visiting scientist at Bartol Research Institute in Delaware University where he engages in the research of the sources of magnetic anomalies on Mars. This position is also associated with Goddard Space Flight Center, NASA, Maryland. He received a doctorate in geophysics from University of Minnesota.

Norman F. Ness is professor at the Bartol Research Institute of the University of Delaware. He received Ph.D. at Massachusetts Institute of Technology in 1959.

P. J. Wasilewski is in the Astrochemistry Branch of the Laboratory for Extraterrestrial Physics at the Goddard Space Flight Center. He received his DrSc from University of Tokyo.

Jack E. P. Connerney joined the Goddard Space Flight Center in 1979 and become an active participant in space magnetic field investigations.

Mario H. Acuña received his PhD in space physics from The Catholic University of America, Washington, DC (1974). Since 1969 he has been associated with NASA’s Goddard Space Flight Center in Greenbelt, MD.

Corresponding author: gunther.kletetschka@gsfc.nasa.gov